Joule

CellPress

Article

A General Method for Regenerating Catalytic Electrodes

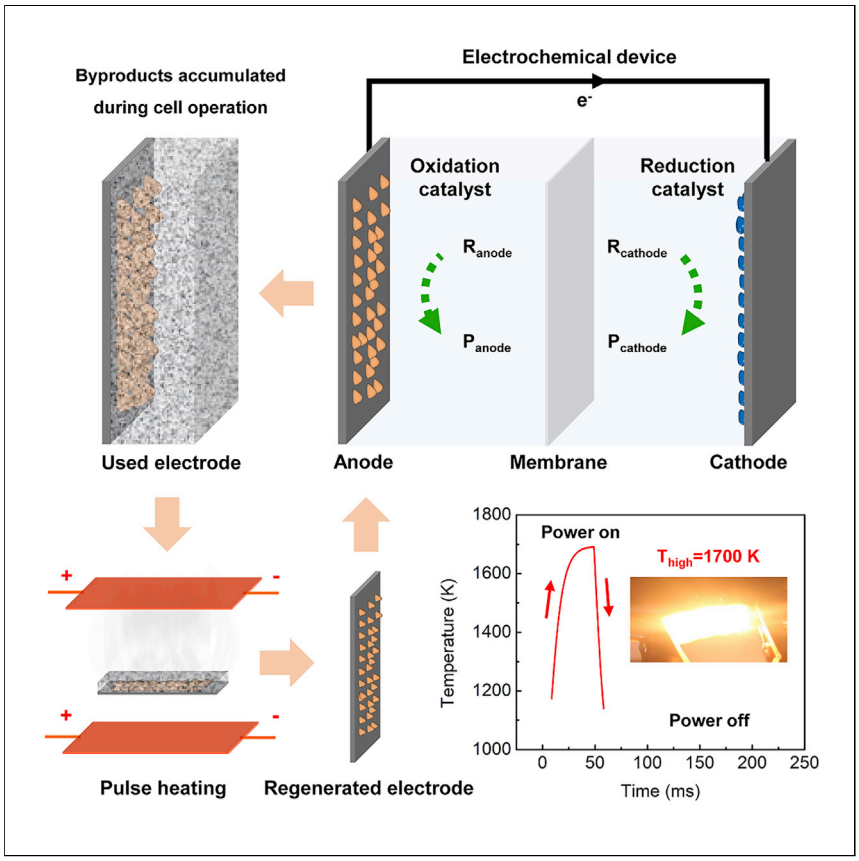

After the prolonged operation of electrochemical cells, byproducts are accumulated, which block the active electrode surface as well as the catalyst. A Joule heating device is designed to conduct high-temperature pulse annealing for regenerating catalytic electrodes. A single electrical pulse is applied to the carbon heating elements to rapidly ramp the temperature up to ~1,700 K and cooled down to room temperature within milliseconds. The non-destructive regeneration process allows for the direct reuse of catalytic electrodes.

Qi Dong, Tangyuan Li, Yonggang Yao, ..., Dunwei Wang, Bao Yang, Liangbing Hu

binghu@umd.edu

HIGHLIGHTS

High-temperature pulse annealing is developed for regenerating catalytic electrodes

The non-destructive treatment allows for the direct reuse of catalytic electrodes

The regeneration can be applied to a variety of carbonaceous and metallic substrates

Dong et al., Joule 4, 2374–2386
November 18, 2020
https://doi.org/10.1016/j.joule.2020.08.008

CellPress

Joule

Article

A General Method for Regenerating Catalytic Electrodes

Qi Dong,[1,5] Tangyuan Li,[1,5] Yonggang Yao,[1] Xizheng Wang,[1] Shuaiming He,[1] Jingyi Li,[2] Jingru Luo,[2] Haochuan Zhang,[2] Yong Pei,[3] Chaolun Zheng,[3] Min Hong,[1] Haiyu Qiao,[1] Jinlong Gao,[1] Dunwei Wang,[2] Bao Yang,[3] and Liangbing Hu[1,4,6,*]

SUMMARY

Catalytic electrodes play an indispensable role in electrochemical devices. As the pursuit of high activity dominates the research focus, limited attention was paid to the recycling technologies. Existing methods often only allow for recovering specific metallic substance without restoring the functionality of the electrode. Herein, we report a general, non-destructive method based on high-temperature pulse annealing to enable direct reuse of catalytic electrodes. The high temperature ensures complete decomposition of byproducts; meanwhile, the rapid annealing maintains the original physiochemical property, and thus the performance of the catalyst. Using the Li-air battery as a model system, we can regenerate a Ru-loaded electrode for 10 times after each cycling operation, thus extending its lifetime by nearly 10 folds. Our method can be readily applied to other electrochemical systems where catalytic electrodes are prone to deactivation by byproducts. This study paves a new way toward highly sustainable operation of electrochemical devices.

INTRODUCTION

The development of electrochemistry has led to the prosperity of various electrochemical technologies, including fuel cells, electrolyzers, batteries, organic electro-synthesis, and so on.[1–5] The operation of many, if not all, necessitates catalytic electrodes to promote desired reactions either on the cathode or the anode or both. Catalysts are mainly based on transition metal or even noble metal elements, which are expensive and environmentally hazardous if not properly treated.[6,7] Compared with the dominant pursuit of the catalytic activity, the sustainability aspect of electrochemical systems has been unfortunately overlooked.[2,7,8] Upon intensive operation, byproducts from the decomposition of the reactant, the carbon electrode and/or the electrolyte would deactivate the electrode surface and degrade its performance.[9–12] Large amounts of electrochemical devices have been disposed due to their limited lifetime without an appropriate recycling treatment.[6] Existing recycling methods, such as pyrometallurgical extraction, hydrometallurgical extraction, and pyro-hydrometallurgical extraction, followed by leaching, purification, separation, and re-synthesis, only extract specific metallic components by destroying the major part of the electrode.[13,14] In comparison, the underdeveloped regeneration technologies (i.e., non-destructive recycling methods), such as hydrothermal treatment, calcination, and chemical coating, hold better promise for future practice, which allows for the direct reuse of the catalytic electrode.[8,13] While the idea of directly regenerating and reusing catalytic electrodes has been proposed and attempted, there still lacks an effective and general approach in

Context & Scale

Despite the fast development of electrochemical energy conversion and storage technologies, the recycling and regeneration methods for used electrochemical devices remain limited. Conventional approaches such as pyrometallurgical and hydrometallurgical extractions can only recover specific metallic components while destroying the rest part of the electrode. Efficient non-destructive regeneration methods are therefore urgently needed. Herein, we report a general regeneration method that allows for direct reuse of catalytic electrodes. Our method involves a high-temperature rapid pulse annealing process for the used catalytic electrode. Our method not only decomposes the byproducts that accumulate on the electrode surface but also restores the original properties of the catalyst. Using the Li-air battery as a model system, we demonstrate that the Ru-loaded electrode can be regenerated for 10 times after each battery-cycling operation to fully recover the electrode performance.

both research and practice beyond the conventional methods, which are often energy intensive and time consuming.

Herein, we report a highly effective technique featuring high-temperature pulse annealing for the direct regeneration of catalytic electrodes. Our approach is enabled by Joule heating of carbon materials to rapidly ramp up the used catalytic electrode to high-temperature and quench down to room temperature within milliseconds.[15,16] The whole regeneration process thus takes only tens of millisecond to complete but can significantly extend the lifetime of the electrodes by many folds. The high temperature contributes to the complete removal of byproducts and contaminations through decomposition and/or evaporation, thereby recovering the active electrode surface; meanwhile, the rapid annealing maintains the original physiochemical property and thus the performance of the catalyst. Using the Li-air battery as a model system, we show that a used Ru-loaded carbonaceous electrode can be directly reused 10 times after each regeneration. The lifetime of the Li-air battery test cell was therefore extended from ca. 200 h to ca. 2,000 h, with comparable overpotential and capacity after each round of recycling. Our method can be readily expanded to other electrochemical systems, where the catalytic electrodes are prone to deactivation by byproducts and contaminations.[1,9–12,17] Compared with the existing wet chemistry method, this study presents a new route toward directly reusing catalytic electrodes for electrochemical devices in a highly sustainable manner.

RESULTS AND DISCUSSION

Figure 1A schematically showcases the configuration of a typical electrochemical cell employing a catalytic electrode and its degradation process. Upon prolonged operations, the byproducts and contaminations resulted from side reactions of the reactants, the carbonaceous electrode, and the electrolyte accumulate onto the electrode that block the active electrode surface as well as the catalyst. To regenerate such an electrode, a Joule heating device is designed to conduct high-temperature pulse annealing (Figure 1B).[15,16] Two pieces of carbon paper are stacked with close proximity and connected with inert electrical wires as the heating element. The used electrode is extracted from the electrochemical cell, separated from the electrolyte, and is then placed between the carbon papers without further pretreatment. A single electrical pulse is applied to the carbon papers from an outside power supply to heat up the whole regeneration device. Owing to the low heat capacity of the carbon heaters, the whole device can be rapidly ramped up to ca. 1,700 K and cooled down to room temperature within tens of millisecond (Figure 1C).[14,16] Using a transient thermal model, we confirmed that the temperature profile of the sandwiched electrode closely follows that of the carbon paper heater (Figure S1). The regeneration temperature can be adjusted in a wide range by tuning electrical parameters (Table S1) to reach desired temperatures. Such tunability can potentially tailor thicker electrodes when thermal inertia becomes large (Figure S2). The Joule heating device operates in an inert atmosphere (e.g., in Ar), and therefore, the carbon heaters are stable for over 10,000 times of pulse operation. The whole device is also scalable according to the size of the used electrode (Figure S3).

Using Li-air battery as a model system, we demonstrate the utility of the regeneration device on a widely studied Ru-loaded catalytic electrode (if not otherwise noted, the catalytic electrode refers to the cathode in the Li-air battery test cell).[18–20] The Li-air battery holds great promise as a leading post-Li-ion energy storage candidate, whose energy density surpasses at least three times of the state-of-the-art Li-ion

[1]Department of Materials Science and Engineering, University of Maryland, College Park, MD 20742, USA

[2]Chemistry Department, Boston College, Chestnut Hill, MA 02467, USA

[3]Department of Mechanical Engineering, University of Maryland, College Park, MD 20742, USA

[4]Center for Materials Innovations, University of Maryland, College Park, MD 20742, USA

[5]These authors contributed equally

[6]Lead Contact

*Correspondence: binghu@umd.edu

https://doi.org/10.1016/j.joule.2020.08.008

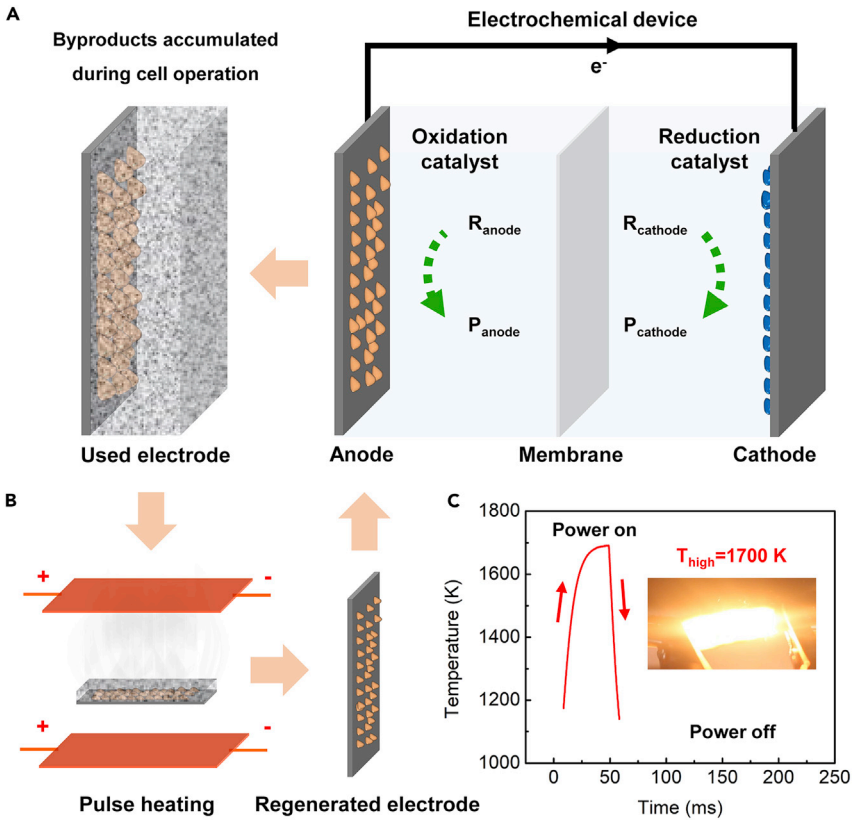

Figure 1. Schematic of the Regeneration Process

(A) Electrochemical cells suffer from byproduct accumulation and contaminations on the electrode upon prolonged operation to convert reactants (R) to products (P), during which the catalysts (yellow and blue particles) are deactivated.

(B) The regeneration device is composed of two pieces of carbon paper, which are used as Joule heating elements to sandwich a used electrode in the middle. After regeneration, the electrode surface is re-exposed, and the catalysts are restored for the direct reuse.

(C) The carbon heaters feature rapid ramping and cooling rates (ca. 10^4 K/s), which are suitable for catalytic electrode regeneration.

cells.[12,21–24] The operation of the Li-air battery heavily relies on catalysts to reduce the overpotentials and improve the round-trip energy efficiency.[25,26] The use of catalysts, however, also exacerbates the degradation of a carbon electrode and an organic electrolyte, which leads to the accumulation of byproducts.[12,27,28] These byproducts gradually deactivate the electrode surface, reduce the activity of the catalyst, and eventually terminate the cell lifetime.[12] Such a problem is not limited to Li-air batteries but is widely shared by a number of electrochemical devices.[8–11] For Li-air batteries, in particular, the cell lifetime is usually limited to ca. 40 cycles at practical current densities, while the commercial Li-ion cells can reach up to 400 cycles at a comparable rate.[25] Other than improving the stability of the electrode and electrolyte, extending the lifetime of Li-air batteries can rely on a viable regeneration method to recover the catalytic electrodes. As such, we see that the Li-air battery can be regarded as a suitable platform to test the utility of our regeneration technique.

The Ru-loaded catalytic electrode was first cycled in a standard Li-air battery testing configuration (Figure S4) with a cutoff capacity of 500 mAh/g_{carbon}. After ca. 40

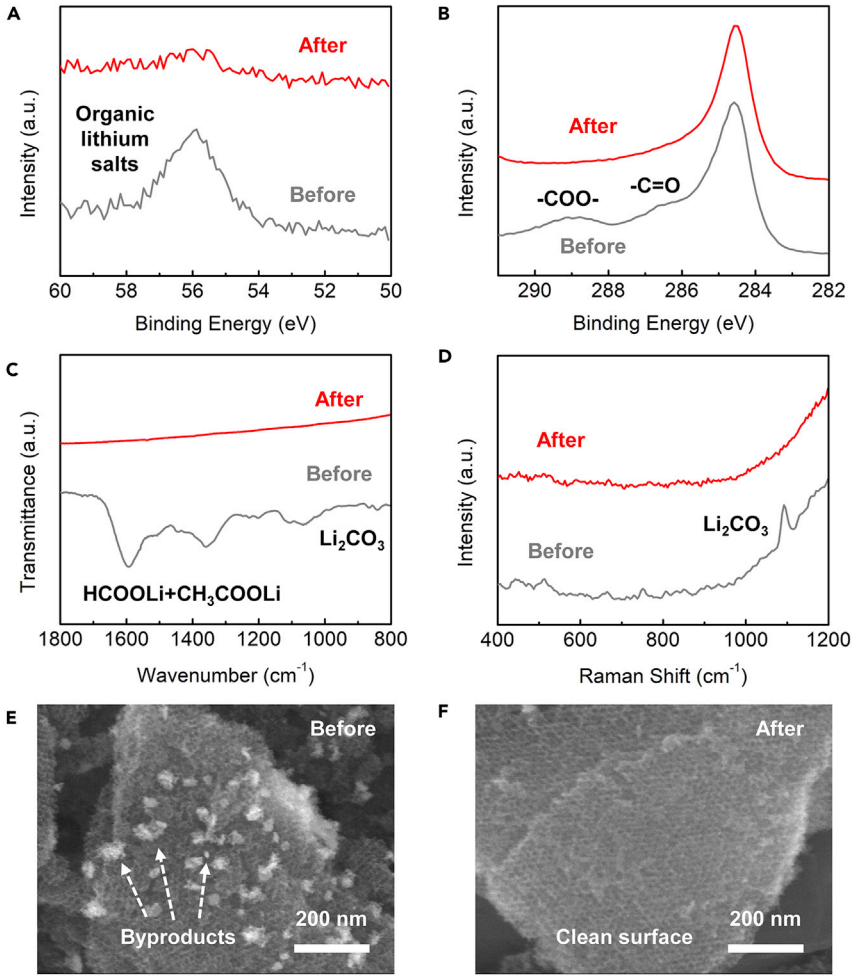

Figure 2. Characterization of the Ru-Loaded Catalytic Electrode

(A) XPS Li 1s spectra before and after regeneration.

(B) XPS C 1s spectra before and after regeneration.

(C) ATR-FTIR spectra before and after regeneration.

(D) Raman spectra before and after regeneration.

(E) SEM image of the used Ru-loaded electrode after cycling, before regeneration. Scale bar, 200 nm.

(F) SEM image of the used Ru-loaded electrode after regeneration. Scale bar, 200 nm.

cycles (corresponding to ca. 200 h of operation), the test cell no longer provides the same discharge capacity in the voltage window (i.e., 2.0 to 4.6 V versus Li^+/Li, Figure S1). The composition of the accumulated byproduct was systematically investigated after extracting the Ru-loaded electrode from the test cell. X-ray photoelectron spectroscopy (XPS) was first employed to analyze the electrode surface (Figure 2A, bottom trace). The Li 1s scan reveals the presence of Li-containing byproducts with a converged peak centering at 56 eV.[29] The C 1s scan indicates the existence of –COO– (~289 eV) and –C=O (~286.7 eV) groups, which correspond to formate and acetate anions in the Li-containing byproducts (Figure 2B, bottom trace).[30] The analysis by ATR-FTIR indicates that lithium carbonate (Li_2CO_3), lithium formate (HCOOLi), and lithium acetate (CH_3COOLi) exist on the cycled electrode (Figure 2C, bottom trace).[31] Li_2CO_3 signal can also be found by Raman spectroscopy (Figure 2D, bottom trace), which exhibits a signature band centered at 1,091 cm^{-1}.[32]

These results together confirm that the byproduct accumulated on the cathode upon cycling operation are Li_2CO_3 and organic lithium salts (i.e., HCOOLi and CH_3COOLi).

Note that the boiling points and decomposition temperatures of HCOOLi, CH_3COOLi, and Li_2CO_3 are up to ca. 1,600 K (Table S2).[33] The pulse peak temperature should be higher than that for a good regeneration effect. The used Ru-loaded catalytic electrode was then applied to test the regeneration device. Referring to the calibrated electrical parameters (Table S1), a pulse duration of 55 ms and a pulse peak temperature of 1,700 K was applied. After the pulse annealing regeneration treatment, the same spectroscopic tools were employed to analyze the electrode. All HCOOLi, CH_3COOLi, and Li_2CO_3 species were completely removed, whose footprints were not detected by XPS, ATR-FTIR, and Raman altogether (Figures 2A–2D, top traces).[29–32] We then compared the morphology of the used electrode by scanning electron microscope (SEM), where a large amount of byproducts can be visualized only after cycling but not after the regeneration treatment (Figures 2E and 2F). These evidences strongly support that our method of using the high-temperature pulse annealing with electrified carbon heaters is effective in cleaning up the used catalytic electrode.

In addition to the complete removal of byproducts to clean up the electrode surface, another key criterion of regeneration is to restore the original physiochemical properties of the catalyst. Transmission electron microscope (TEM) was used to track the morphological evolution of the Ru catalyst before using for the Li-air battery cycling (in the pristine state) and after regeneration. Comparing with the morphology of the cathode in the pristine state (Figure 3A), no agglomeration of Ru catalyst was observed in the regenerated state (Figure 3B). Scanning transmission electron microscope (STEM) images with better contrast confirmed the nearly identical particle size and distribution of the Ru nanoparticles in the pristine (Figures 3C and 3E) and recycled states (Figures 3D and 3F). Note that the pulse peak temperature and the pulse duration both play critical roles in this process. Temperatures that are too low will not have sufficient driving force to remove the byproducts completely, while those that are too high will change the structure of the electrode (Figure S6).[34] Transient pulse duration is important to prevent catalyst agglomeration. We found that the pulse duration of 55 ms preserved the original morphology of the Ru catalyst, beyond which severe ripening of Ru into large particles would occur driven by the surface energy (Figures S7 and S8). The increased size of Ru catalyst is not desirable, as it will reduce the aspect ratio and therefore undermine its catalytic performance.[18,34,35]

The regenerated catalytic electrode was applied to the identical Li-air battery setup for another round of cycling tests. Compared with the cycling profile when the electrode was in its pristine state, (Figure 4A), the regenerated electrode (denoted as "Regeneration-1," or "R-1") showed comparable overpotentials and cycle lifetime (Figure 4B). The same regeneration process was then repeated for another 9 times after each cycling operation. The representative cycling profiles at the 2^{nd}, 5^{th}, and 10^{th} regeneration rounds (denoted as "Regeneration-2," "Regeneration-5," and "Regeneration-10") are shown in Figures 4C–4E, respectively. The overpotentials in these representative traces are by and large comparable, which suggests that the catalytic activity of the Ru-loaded electrode can be restored to its original state. In addition, the cycle numbers (e.g., 40 cycles) are also comparable among all 10 regeneration rounds, further indicating that the performance of the electrode has been recovered. Through multiple rounds of regeneration, the total lifetime of

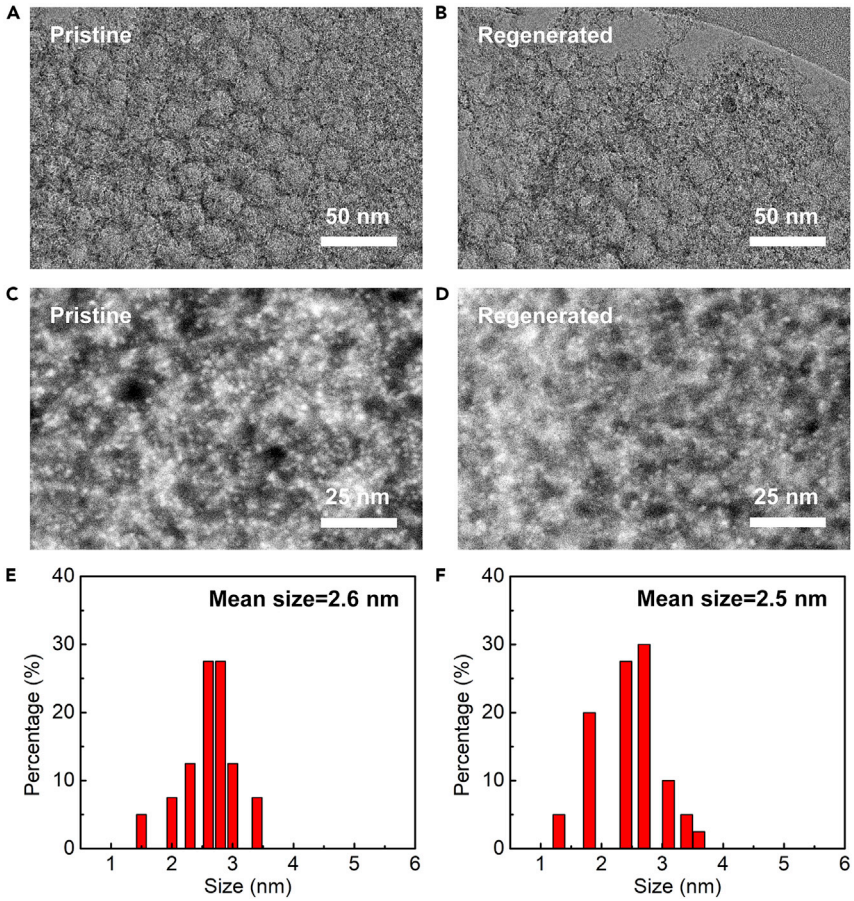

Figure 3. Characterization of the Ru Catalyst

(A and B) TEM images of the Ru-loaded electrode at pristine state before using (A) and after cycling followed by regeneration (B). Scale bar, 50 nm.

(C–F) STEM images of the Ru-loaded electrode at pristine state before using (C) and after cycling followed by regeneration (D), scale bar, 25 nm, along with the corresponding Ru particle size distribution shown in (E) and (F), respectively. The black dots in (A) and (B), the white dots in (C) and (D) correspond to the Ru catalyst.

the Li-air test cell was extended from ca. 40 cycles to ca. 400 cycles, translating to a lifetime increase from ca. 200 h to ca. 2,000 h.

Note that such a desirable regeneration performance by our high-temperature pulse annealing technique cannot be reproduced by the conventional wet chemistry method. Using an electrode that was cleaned by acid treatment in a freshly assembled cell, the device lasted only for four additional cycles and quickly reached the lower cutoff voltage during discharge (Figure 4F). Spectroscopic analysis indicates that the footprints of the major byproducts have not been fully removed on the acid-treated electrode (Figures S9 and S10).[30,31] We hypothesize that the hydrophobicity of carbonaceous electrodes (e.g., 3DOm carbon and carbon paper) induce poor contact between the byproducts and the proton. In addition, poor mass transport may play an important role to undermine the regeneration performance through acid rinsing, as the electrode is highly porous. Together, these factors led to the undesired regeneration effect by acid treatment. It is noteworthy that prolonged soaking or sonication in an acidic environment could potentially improve the regeneration effect. However, these conditions inevitably incur detrimental

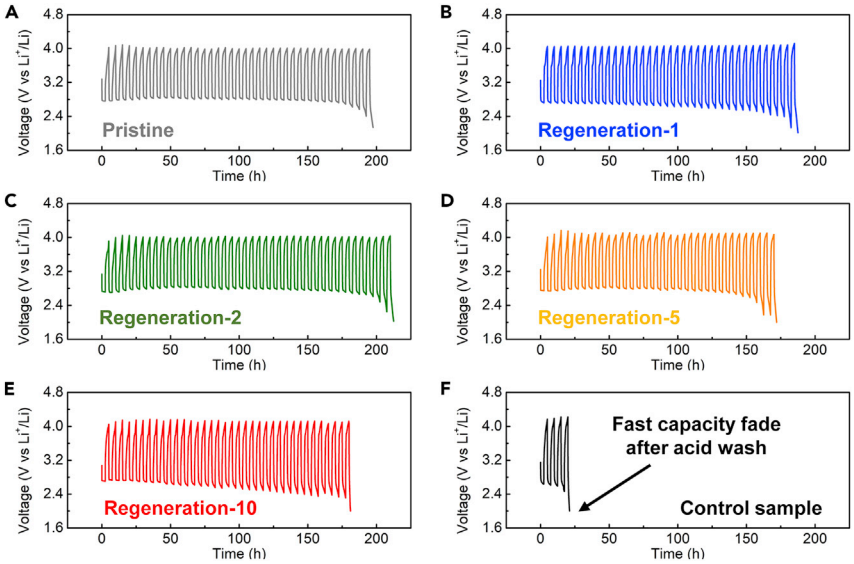

Figure 4. Cycling Performance of the Ru-Loaded Catalytic Electrode in Li-air Batteries Using a 500 mAh/g_{carbon} Cutoff Capacity at a Current Density of 200 mA/g_{carbon}

(A) Cycling performance of the Ru-loaded electrode in the pristine state.

(B) Cycling performance of the used Ru-loaded electrode after the 1st regeneration.

(C) Cycling performance of the used Ru-loaded electrode after the 2nd regeneration.

(D) Cycling performance of the used Ru-loaded electrode after the 5th regeneration.

(E) Cycling performance of the used Ru-loaded electrode after the 10th regeneration.

(F) Cycling performance of the used Ru-loaded electrode after the wet chemistry method featuring acid treatment.

effects on the structural as well as the chemical stability of the catalytic electrode. This set of data indicates that the conventional recycling treatment by wet chemistry does not permit direct reuse of the catalytic electrode. Our regeneration method, on the other hand, offers precise control over temperature and timescale, and therefore, for the first time, allows for the direct reuse of catalytic electrode and significantly extends its lifetime in electrochemical devices to the best of our knowledge.

Despite the promising regeneration performance, we are mindful of the potential confounding factors that could complicate the data interpretation. A few possible alternative explanations for the resumed electrode performance need to be ruled out by additional experimental evidence. First, the carbon substrate could be recrystallized and the defects could be healed by multiple rounds of high-temperature treatment.[15,16] It has been reported that the defective sites of carbon can serve as the starting point for the parasitic chemical reactions that result in poor stability and low cyclability for Li-air batteries.[36] As a result, healing defective sites during multiple rounds of pulse annealing may lead to an improved or even resumed cyclability. To exclude this confounding factor, Raman spectroscopy and X-ray diffraction (XRD) were employed to track the structural evolution of the carbonaceous substrate. The D/G ratios of the regenerated Ru-loaded carbon electrode after various regeneration rounds remained nearly identical (Figure 5A). The XRD pattern of the regenerated Ru-loaded carbon electrode also changed insignificantly among various rounds of the pulse annealing treatment (Figure 5B). These results suggest that the transient heating at 1,700 K was only sufficient for the removal of byproducts but was not capable of dramatically altering the structure or the chemical nature of the carbonaceous substrate.

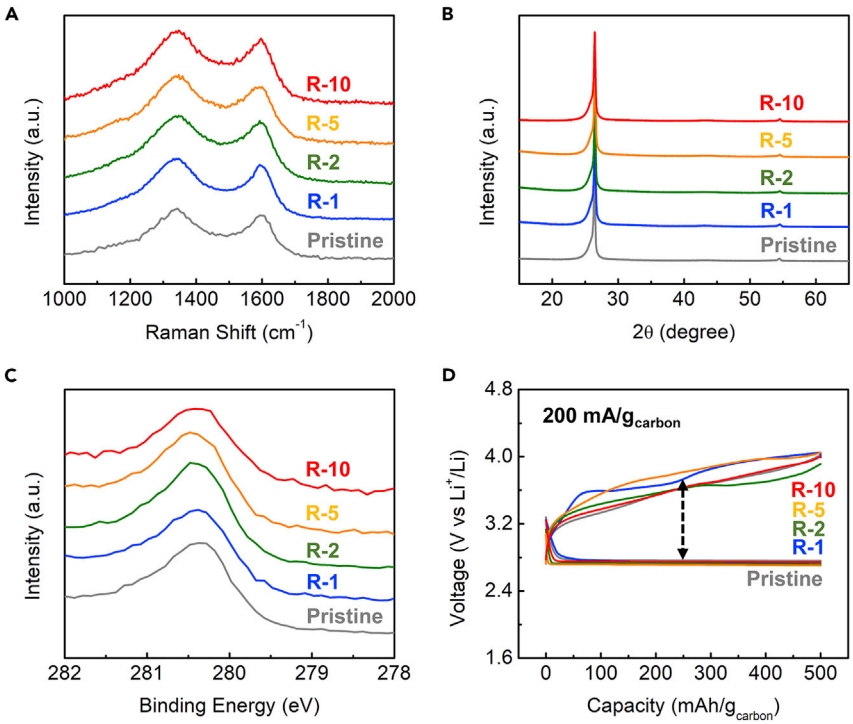

Figure 5. Additional Characterizations during Multiple Rounds of Electrode Regeneration

(A) Raman analyses on the Ru-loaded carbon electrode upon multiple rounds of regeneration.

(B) XRD analyses on the Ru-loaded carbon electrode upon multiple rounds of regeneration.

(C) XPS analyses on the Ru 3d spectra upon multiple rounds of regeneration.

(D) Discharge and recharge profiles during the 1st cycle of the Li-air battery test cell at representative regeneration rounds. The discharge profiles are nearly identical, and the recharge profiles show reasonable overpotential variations within ca. 200 mV.

Second, despite using an inert environment for the regeneration process, the oxidation state or the bonding environment of the catalyst may vary due to the high-temperature treatment. Such a change may also influence the cell performance in an unpredictable manner.[19] In order to rule out this factor, XPS analyses were performed, which revealed a minimal shift of the Ru peak among multiple rounds of regeneration (Figure 5C).[34] In addition, the initial Li-air cell discharge and recharge profiles upon various rounds of regeneration showcase comparable overpotentials (Figure 5D), which suggests that the cell operations are likely regulated by the catalysts with the same physiochemical nature and comparable loading (Figure S11). We further conducted qualitative product analysis to confirm that the operation of the Li-air battery was indeed based on Li_2O_2 chemistry in our study. Discharge products that are similar in size and shape (i.e., the typical toroidal morphology) were observed by SEM for the Ru-loaded electrode during the first-time cycling and the regenerated Ru-loaded electrode during the new cycling operation (Figure S12).[25] Note that while the regeneration treatment does not change the physiochemical properties of the Ru catalyst, the regeneration effect through decomposition and/or evaporation does not rely on the Ru catalyst either (Figure S13). Taken together, the above pieces of evidence not only exclude other confounding factors but also strongly support the utility of our high-temperature pulse annealing method for regenerating catalytic electrodes.

Our regeneration method is not limited to the carbonaceous electrode. To demonstrate its universality, we tested another model system featuring Ti-mesh-supported Pt

nanoparticle catalyst (Figure S14), which can be employed for alcohol fuel cells, biomass electrolyzers, organic electro-synthesis, and so on. To simulate the byproduct accumulation, we artificially introduced a Li_2CO_3 coating by drop casting its ethanol solution on the electrode followed by vacuum drying. Li_2CO_3, thus mimicking one universal byproduct formed via the decomposition of electrolyte, electrode, and/or active materials during the operation of the aforementioned electrochemical devices. ATR-FTIR and SEM were employed to track the artificial byproduct (i.e., Li_2CO_3) and the distribution of Pt nanoparticles upon high-temperature pulse annealing, respectively. Using the same parameters for regenerating the carbonaceous electrode, a good regeneration effect can be reproduced in this model system as well. In particular, the footprints of Li_2CO_3 were not detected after regeneration, indicating the complete removal of byproduct at high-temperatures (Figure S15); meanwhile, the Pt nanoparticles remained well-dispersed without noticeable aggregation, which supports the critical role of the transient duration for pulse annealing (Figure S16). Using ethanol oxidation reaction as a proof-of-concept,[30] we showed that the regenerated electrode exhibited comparable cyclic voltammetry features as well as a nearly identical stability in the chronoamerometry test with the pristine electrode under the same testing conditions (Figure S17). These results confirmed that our high-temperature pulse annealing can be a general method for regenerating catalytic electrodes.

Conclusion

In summary, we demonstrate a general approach based on the high-temperature pulse annealing technique to regenerate and directly reuse catalytic electrodes in electrochemical devices. Our regeneration treatment not only removes the byproducts and contaminations to clean up the electrode but also resumes the original properties of the catalyst. High-temperature is critical for the complete removal of the byproducts and contaminations; meanwhile, the transient heating duration ensures no catalyst agglomeration or other parasitic processes. Using the Li-air battery as a model system, the Ru-loaded catalytic electrode can be regenerated for 10 times, which extends the lifetime of the Li-air battery by nearly 10 folds. Our method is not limited to metal-air batteries but can be readily extended to a variety of electrochemical devices, such as direct alcohol fuel cells, organic electro-synthesis, CO_2 and biomass electrolyzers, and so on. Compared with a conventional wet chemistry recycling method that can only recover specific metallic elements at the expense of other parts of the electrode, this study offers a new way to regenerate catalytic electrode for a broad range of applications.

EXPERIMENTAL PROCEDURES

Resource Availability

Lead Contact

Further information and requests for resources and materials should be directed to and will be fulfilled by the Lead Contact, Liangbing Hu (binghu@umd.edu).

Materials Availability

This study did not generate new unique materials.

Data and Code Availability

This study did not generate code. The data supporting the current study are available from the Lead Contact on reasonable request.

Starting Materials and Instruments

Lithium bis(trifluoromethane)sulfonimide (LiTFSI, ≥99.9%, extra dry) was obtained from Solvay. 1,2-dimethoxyethane (DME, anhydrous), Li ribbon (≥ 99.9%, trace

metals basis, 0.38 mm), lithium carbonate (Li_2CO_3, ≥99.0%, reagents grade), and polytetrafluoroethylene (PTFE, 60 wt % aqueous solution) were purchased from Sigma-Aldrich. DME was dried using 4 Å molecular sieves prior to test cell assembly. Deionized water (DI H_2O, 18.2 MΩ•cm) was taken from a Barnstead Nanopure Diamond system. The DME-based electrolyte was prepared by mixing 1 M LiTFSI into the DME after the extra drying process. Carbon paper, which is also called the gas diffusion layer (GDL, Toray 120) was obtained from the Fuel Cell Store. Ti mesh was obtained from Cleveland Wire Cloth. The carbon paper and Ti mesh substrates were washed by acetone, methanol, and isopropanol in sequence, each for 3 times, and were then thoroughly dried under vacuum before use. The three-dimensionally ordered mesoporous (3DOm) carbon was synthesized using the identical process reported by Fan et al.,[37] where the template method was used to yield the porous structure with an inner diameter of ca. 35 nm. Multipurpose copper sheets (99.9%, 0.002" thickness) and wires (99.9%) were purchased from McMaster Carr. A solid-state relay (SSR) device that has DC input and DC output (maximum current 25 A) was purchased from Omega. The electrical input to the SSR was triggered by the Keithley source meter (model 2400). The output signal was used to control a power source (VOLTEQ HY6020EX).

Catalytic Electrode Preparation

The catalytic electrodes used in this study were prepared by the method reported by Lacey et al.[34] In a typical preparation process, the 3DOm carbon with PTFE binder was dispersed into isopropyl alcohol (IPA) with 95:5 mass ratio. The mixture was then drop casted to the carbon paper substrate to reach a loading density of ca. 1.0 mg cm^{-2}. The uniform coverage by 3DOm carbon was confirmed under a microscope before testing. The electrodes were further dried in a vacuum oven under 400 K to remove residual solvents. Then, the 3DOm carbon-loaded carbon paper was wrapped with the copper film and was used to apply current in an Ar-filled atmosphere. The Ru-containing ethanol solution was then drop cast on the samples. After the samples were dried at room temperature, the carbothermal shock process was applied in an Ar-filled glovebox with the DC power supply. A transient pulse current was directly applied to the carbon-loaded substrate in an Ar-filled glovebox to induce the thermal shock. The pulse time was controlled by the SSR, which was triggered by the Keithley source meter. The Pt/Ti mesh electrode was prepared by soaking the Ti mesh substrate with the Pt-containing ethanol solution, followed by vacuum drying. Then a radiation pulse heating via Joule heating of a carbon paper heating element was applied to the Ti mesh to result in the final product.

Reactor Setup and Regeneration Procedure

Two pieces of carbon paper (e.g., made by GDL, carbon nanofiber paper or buckypaper sheets, ca. 1.2 cm × 2 cm)[16] were stacked with close proximity and were connected in parallel with inert electrical copper wires and clips as the heating elements. The high accuracy source meter was used to vary the electrical input for pulse annealing operations. In particular, for a typical pulse duration of 55 ms, various voltages were applied to adjust the temperature of the heating elements and to generate the reference table (Table S1). The speed level "normal" was used to provide the 55 ms pulse duration. For the pulse durations of 110 ms, 550 ms, and 1.1 s, the pulse period was repeated for 2, 10, and 20 times, respectively. After each cycling test, the catalytic electrode was extracted from the cell, washed by DME to remove the residual electrolyte, and then placed in between without further pretreatment. A specific pulse signal was applied to the two carbon papers through the electrical power source to heat up the whole regeneration device. After pulse annealing, the electrode was ready to be reused in another electrochemical device

as a "fresh" sample. The regeneration of Pt/Ti mesh electrode and bare 3DOm carbon (in the absence of Ru catalyst) with the artificial byproduct of Li_2CO_3 (by drop casting its ethanol solution followed by vacuum drying) adopted the same regeneration procedure and parameters. For the recycling by a conventional wet chemistry method, the cycled catalytic electrode was soaked in 1 M HCl for 1 h, and rinsed with DI water and DME, followed by vacuum drying before further test.

Temperature Acquisition

The temperature profile of the carbon-based heating element was calibrated using a Vision Research Phantom Miro M110 high-speed camera.[38] The temperature was simulated via gray-body assumption.[39] The calibration was completed by a Newport Oriel 67000 Series Blackbody Infrared Light Source. For each pixel, to recover the values for the red, green, and blue channels, MATLAB was used to demosaic the information with the camera's Bayer color filter array. The temperature was estimated in a way that three-color ratios were applied simultaneously via minimizing their summed error with the error threshold to approximately 110 K. For the resulted temperature curve, only unsaturated pixels within the error threshold and above the black level were included to generate the temperature for a contiguous area of at least 10 acceptable pixels. The high temperature of the pulse annealing device was calculated by fitting the emitted light intensity based on gray-body radiation.

Spectroscopic and Microscopic Characterizations

Prior to the spectroscopic and microscopic characterizations, the used catalytic electrodes were extracted from the test cell, washed with DME for 3 times to remove remaining supporting salts, and then dried in air. XPS was conducted using a Thermo Scientific K-Alpha+ system with an Al X-ray source. SEM was conducted with a JEOL 6340F microscope with the accelerating voltage of 5 and 10 kV. The TEM samples were prepared by sonicating the catalytic cathode samples in ethanol to disperse the Ru-loaded 3DOm carbon powders for 30 min, then drop cast the solution onto a TEM grid. The TEM and STEM images were captured by JEOL JEM 2100 FEG-TEM at 200 kV. XRD characterization was completed using a PANalytical X'Pert Pro diffractometer with Cu Kα radiation. Raman spectra were collected using a micro-Raman system (XploRA, Horiba), which was equipped with a 532 nm laser excitation. The ATR-FTIR spectra were collected using a Thermo Nicolet NEXUS 670 instrument. Particle size distribution was conducted by measuring and plotting based on the exact size (rather than equal size range) of 40 particles in each image to better reflect the statistical information, especially the mean size.

Electrochemical Characterization

All electrochemical data in this study were collected using a VMP3 potentiostat (Bio-Logic) and with a home-designed Swagelok-type test cell.[29] The cell assembly was all conducted in an Ar-filled and O_2-tolerant glovebox (Mbraun, H_2O <0.1ppm) at room temperature (303 K). The Li-air test cells were assembled with a 2-electrode configuration. The Ru-loaded 3DOm carbon supported on carbon paper was applied as the cathode. Lithium ribbon with an area of ca. 1 cm^2 was applied as the anode. Two pieces of separators made of polypropylene were applied in the middle. The current density and capacity were normalized to the applied weight of the 3DOm carbon. In a typical assembly, 200 μL DME-based electrolyte was injected to each Li-air test cell. After assembly, high purity O_2 (Airgas) was forced through the headspace of the Swagelok-type cell at 20 sccm for 60 s. The assembled cell was then separated from the O_2 line and equilibrated to ambient pressure. The cycling operation for the catalytic cathode was conducted at 200 mA g_{carbon}^{-1} with a cutoff capacity of 500 mAh g_{carbon}^{-1} (operated for 5 h per cycle, 2.5 h for discharge

and recharge). Electrochemical ethanol oxidation reaction was performed using Pt/Ti mesh as the working electrode in a solution containing 1.0 M KOH and 1.0 M ethanol. The cyclic voltammograms were collected using a scan rate of 25 mV/s. The chronoamerograms were collected at −0.25 V versus SCE.

Modeling of the Temperature Profile of the Used Electrode during Regeneration

A transient thermal model is developed using ANSYS to study the temporal and spatial temperature profile of the sample. The material and geometrical properties of the sample are listed in Table S3.[40] Since the sample has a high porosity and a surface roughness, it is assumed that there is an 8 μm thermal contact layer between the sample and each carbon paper heater. The contact layer is assumed to have the same thermal properties as the sample, except that its thermal conductivity is conservatively assumed to be only 0.85 W/m/K. The temporal temperature profile of the heaters is extracted from the experimental data. The heat conduction in the sample is assumed to be one dimensional since the thicknesses considered are much smaller than the width and length, thus for a sample with a larger area such as 85 mm × 50 mm as used in Figure S3, the temperature distribution would be the same.

SUPPLEMENTAL INFORMATION

Supplemental Information can be found online at https://doi.org/10.1016/j.joule.2020.08.008.

ACKNOWLEDGMENTS

This study has no direct funding support. The Li-air battery efforts are supported by NSF (CBET 1804085). We acknowledge the support from Maryland NanoCenter, the Surface Analysis Center, and the AIM Lab. XPS was conducted at the Center for Nanoscale Systems at Harvard University. We thank Prof. Michael R. Zachariah and Dylan J. Kline for their assistance with the temperature measurement. We thank Prof. Wei Fan and Dr. Vivek Vattipalli for providing the 3DOm carbon. We thank Dr. Yumin He for helping with the schematic.

AUTHOR CONTRIBUTIONS

L.H., Q.D., and Y.Y. came up with the design concept. Q.D. performed most of the experiments. T.L. and J.G. assisted with the regeneration. X.W. and T.L. conducted the temperature measurement. S.H. and J.Li. carried out ATR-FTIR measurement. J.Luo., H.Z., H.Q., and D.W. helped with the electrochemical measurements. Y.P., C.Z., and B.Y. conducted the thermal modeling. M.H. carried out the statistical analyses on the Ru nanoparticles. Q.D. designed the schematic figure. All authors participated in data interpretation. Q.D. wrote the paper together with input from all authors. L.H. supervised the project.

DECLARATION OF INTERESTS

The authors declare no competing interests.

Received: May 17, 2020
Revised: July 8, 2020
Accepted: August 14, 2020
Published: September 14, 2020

REFERENCES

1. Li, Y.G., and Lu, J. (2017). Metal-air batteries: will they be the future electrochemical energy storage device of choice? ACS Energy Lett *2*, 1370–1377.
2. Pehnt, M. (2001). Life-cycle assessment of fuel cell stacks. Int. J. Hydr. Energ. *26*, 91–101.
3. Mohammadi, A., and Mehrpooya, M. (2018). A comprehensive review on coupling different types of electrolyzer to renewable energy sources. Energy *158*, 632–655.
4. Kingston, C., Palkowitz, M.D., Takahira, Y., Vantourout, J.C., Peters, B.K., Kawamata, Y., and Baran, P.S. (2020). A survival guide for the "electro-curious. Acc. Chem. Res. *53*, 72–83.
5. Dong, Q., Zhang, X., He, D., Lang, C., and Wang, D. (2019). Role of H2O in CO2 electrochemical reduction as studied in a water-in-salt system. ACS Cent. Sci. *5*, 1461–1467.
6. Ramesh Babu, B., Parande, A.K., and Ahmed Basha, C. (2007). Electrical and electronic waste: a global environmental problem. Waste Manag. Res. *25*, 307–318.
7. Duclos, L., Lupsea, M., Mandil, G., Svecova, L., Thivel, P.-X., and Laforest, V. (2017). Environmental assessment of proton exchange membrane fuel cell platinum catalyst recycling. J. Clean. Prod. *142*, 2618–2628.
8. Chen, M., Ma, X., Chen, B., Arsenault, R., Karlson, P., Simon, N., and Wang, Y. (2019). Recycling end-of-life electric vehicle lithium-ion batteries. Joule *3*, 2622–2646.
9. Burstein, G.T., Barnett, C.J., Kucernak, A.R., and Williams, K.R. (1997). Aspects of the anodic oxidation of methanol. Catal. Today *38*, 425–437.
10. Wang, C.Y. (2004). Fundamental models for fuel cell engineering. Chem. Rev. *104*, 4727–4765.
11. Siu, J.C., Fu, N., and Lin, S. (2020). Catalyzing electrosynthesis: a homogeneous electrocatalytic approach to reaction discovery. Acc. Chem. Res. *53*, 547–560.
12. Yao, X.H., Dong, Q., Cheng, Q.M., and Wang, D.W. (2016). Why do lithium-oxygen batteries fail: parasitic chemical reactions and their synergistic effect. Angew. Chem. Int. Ed. Engl. *55*, 11344–11353.
13. Cui, J., and Zhang, L. (2008). Metallurgical recovery of metals from electronic waste: a review. J. Hazard. Mater. *158*, 228–256.
14. Fan, E., Li, L., Wang, Z., Lin, J., Huang, Y., Yao, Y., Chen, R., and Wu, F. (2020). Sustainable recycling technology for Li-ion batteries and beyond: challenges and future prospects. Chem. Rev. *120*, 7020–7063.
15. Luong, D.X., Bets, K.V., Algozeeb, W.A., Stanford, M.G., Kittrell, C., Chen, W., Salvatierra, R.V., Ren, M., McHugh, E.A., Advincula, P.A., et al. (2020). Gram-scale bottom-up flash graphene synthesis. Nature *577*, 647–651.
16. Yao, Y., Huang, Z., Li, T., Wang, H., Liu, Y., Stein, H.S., Mao, Y., Gao, J., Jiao, M., Dong, Q., et al. (2020). High-throughput, combinatorial synthesis of multimetallic nanoclusters. Proc. Natl. Acad. Sci. USA *117*, 6316–6322.
17. Qi, M., Dong, Q., Wang, D., and Byers, J.A. (2018). Electrochemically switchable ring-opening polymerization of lactide and cyclohexene oxide. J. Am. Chem. Soc. *140*, 5686–5690.
18. Cheng, F.Y., and Chen, J. (2012). Metal-air batteries: from oxygen reduction electrochemistry to cathode catalysts. Chem. Soc. Rev. *41*, 2172–2192.
19. Dong, Q., and Wang, D.W. (2018). Catalysts in metal-air batteries. MRS Commun *8*, 372–386.
20. Li, F.J., Chen, Y., Tang, D.M., Jian, Z.L., Liu, C., Golberg, D., Yamada, A., and Zhou, H.S. (2014). Performance-improved Li-O2 battery with Ru nanoparticles supported on binder-free multi-walled carbon nanotube paper as cathode. Energy Environ. Sci. *7*, 1648–1652.
21. Abraham, K.M., and Jiang, Z. (1996). A polymer electrolyte-based rechargeable lithium/oxygen battery. J. Electrochem. Soc. *143*, 1–5.
22. Black, R., Adams, B., and Nazar, L.F. (2012). Non-aqueous and hybrid Li-O2 batteries. Adv. Energy Mater. *2*, 801–815.
23. Bruce, P.G., Freunberger, S.A., Hardwick, L.J., and Tarascon, J.M. (2011). Li-O2 and Li-S batteries with high energy storage. Nat. Mater. *11*, 19–29.
24. Girishkumar, G., McCloskey, B., Luntz, A.C., Swanson, S., and Wilcke, W. (2010). Lithium-air battery: promise and challenges. J. Phys. Chem. Lett. *1*, 2193–2203.
25. Lu, Y.C., Gallant, B.M., Kwabi, D.G., Harding, J.R., Mitchell, R.R., Whittingham, M.S., and Shao-Horn, Y. (2013). Lithium-oxygen batteries: bridging mechanistic understanding and battery performance. Energy Environ. Sci. *6*, 750–768.
26. McCloskey, B.D., Scheffler, R., Speidel, A., Bethune, D.S., Shelby, R.M., and Luntz, A.C. (2011). On the efficacy of electrocatalysis in nonaqueous Li-O2 batteries. J. Am. Chem. Soc. *133*, 18038–18041.
27. Lu, Y.C., Gasteiger, H.A., Parent, M.C., Chiloyan, V., and Shao-Horn, Y. (2010). The influence of catalysts on discharge and charge voltages of rechargeable Li-oxygen batteries. Electrochem. Solid-State Lett. *13*, A69–A72.
28. McCloskey, B.D., and Addison, D. (2017). A viewpoint on heterogeneous electrocatalysis and redox mediation in nonaqueous Li-O2 batteries. ACS Catal *7*, 772–778.
29. Dong, Q., Yao, X.H., Zhao, Y.Y., Qi, M., Zhang, X.Z., Sun, H.Y., He, Y.M., and Wang, D.W. (2018). Cathodically stable Li-O2 battery operations using water-in-salt electrolyte. Chem *4*, 1345–1358.
30. Dong, Q., Zhao, Y., Han, X., Wang, Y., Liu, M.C., and Li, Y. (2014). Pd/Cu bimetallic nanoparticles supported on graphene nanosheets: facile synthesis and application as novel electrocatalyst for ethanol oxidation in alkaline media. Int. J. Hydr. Energ. *39*, 14669–14679.
31. Freunberger, S.A., Chen, Y., Drewett, N.E., Hardwick, L.J., Bardé, F., and Bruce, P.G. (2011). The lithium-oxygen battery with ether-based electrolytes. Angew. Chem. Int. Ed. Engl. *50*, 8609–8613.
32. Pasierb, P., Komornicki, S., Rokita, M., and Rękas, M. (2001). Structural properties of Li2CO3-BaCO3 system derived from IR and Raman spectroscopy. J. Mol. Struct. *596*, 151–156.
33. Patnaik, P. (2002). Handbook of Inorganic Chemicals (McGraw-Hill).
34. Lacey, S.D., Dong, Q., Huang, Z., Luo, J., Xie, H., Lin, Z., Kirsch, D.J., Vattipalli, V., Povinelli, C., Fan, W., et al. (2019). Stable multimetallic nanoparticles for oxygen electrocatalysis. Nano Lett *19*, 5149–5158.
35. Yao, X.H., Cheng, Q.M., Xie, J., Dong, Q., and Wang, D.W. (2015). Functionalizing titanium disilicide nanonets with cobalt oxide and palladium for stable Li oxygen battery operations. ACS Appl. Mater. Inter. *7*, 21948–21955.
36. Ottakam Thotiyl, M.M.O., Freunberger, S.A., Peng, Z.Q., and Bruce, P.G. (2013). The carbon electrode in nonaqueous Li-O2 cells. J. Am. Chem. Soc. *135*, 494–500.
37. Fan, W., Snyder, M.A., Kumar, S., Lee, P.S., Yoo, W.C., McCormick, A.V., Lee Penn, R., Stein, A., and Tsapatsis, M. (2008). Hierarchical nanofabrication of microporous crystals with ordered mesoporosity. Nat. Mater. *7*, 984–991.
38. Fu, T., Wang, Z., and Cheng, X. (2010). Temperature measurements of diesel fuel combustion with multicolor pyrometry. J. Heat Transfer *132*, 051602.
39. Jacob, R.J., Kline, D.J., and Zachariah, M.R. (2018). High speed 2-dimensional temperature measurements of nanothermite composites: probing thermal vs. gas generation effects. J. Appl. Phys. *123*, 115902.
40. Butland, A.T.D., and Maddison, R.J. (1973). The specific heat of graphite: an evaluation of measurements. J. Nucl. Mater. *49*, 45–56.